# Mechanisms of electroless metal plating: I. Mixed potential theory and the interdependence of partial reactions

by Perminder Bindra
David Light
David Rath

Electroless plating reactions are classified according to four overall reaction schemes in which each partial reaction is either under diffusion control or electrochemical control. The theory of a technique, based on the observation of the mixed potential as a function of agitation, concentration of the reducing agent, and concentration of metal ions, is presented. By using this technique it is shown that in electroless copper plating the copper deposition reaction is diffusion-controlled, while the formaldehyde decomposition reaction is activation-controlled. Values of the kinetic and mechanistic parameters for the partial reactions obtained by this method and by other electrochemical methods indicate that the two partial reactions are not independent of each other.

**°Copyright** 1984 by International Business Machines Corporation. Copying in printed form for private use is permitted without payment of royalty provided that (1) each reproduction is done without alteration and (2) the *Journal* reference and IBM copyright notice are included on the first page. The title and abstract, but no other portions, of this paper may be copied or distributed royalty free without further permission by computer-based and other information-service systems. Permission to *republish* any other portion of this paper must be obtained from the Editor.

### Introduction

The Wagner and Traud [1] theory of mixed potentials has been verified for several corrosion systems [2, 3]. According to this theory, the rate of a faradaic process is independent of other faradaic processes occurring simultaneously at the electrode and thus depends only on the electrode potential. Hence the polarization curves for independent anodic and cathodic processes may be added to predict the overall rates and potentials which exist when more than one reaction occurs simultaneously at an electrode. Wagner and Traud [1] demonstrated the dissolution of zinc amalgam to be dependent on the amalgam potential but independent of the mechanism of simultaneous hydrogen evolution.

More recently, electroless metal plating processes have been identified as mixed potential systems [4, 5], and it has been suggested that the electroless plating mechanisms can be predicted from the polarization curves for the partial processes. Such polarization curves have been obtained by one or more of the following methods: (1) by applying the steady-state galvanostatic or potentiostatic pulse method to each partial reaction separately; (2) by applying potential scanning techniques to a rotating disk electrode; (3) by measuring the plating rate from the substrate weight-gain as a function of the concentration of the reductant or the oxidant [6]. The plating rate is then plotted against the

mixed potential to obtain the Tafel parameter [7, 8]. These methods suffer from the usual limitations associated with the theory of mixed potentials. For example, extrapolation of the polarization curve for the catalytic decomposition of the reducing agent to the plating potential is not valid if the catalytic properties of the surface change with potential over the range of interest. The extrapolation is also not valid if the rate-determining step, and hence the Tafel slope for any process, changes in the potential range through which the polarization curve is extrapolated. Further, at least one of the two partial reactions involved in electroless metal plating can be diffusion-controlled. Therefore, the weight-gain method cannot be used to ascertain the plating mechanism unless the electrochemically controlled partial reaction is first identified.

A further limitation to the extrapolation of polarization curves and to the application of the mixed potential concept to electroless plating that is often not realized [9] is that the two partial processes are not independent of each other. For corrosion processes such a limitation was first discovered by Andersen et al. [10]. In the present study, we have found that the same limitation to the application of the mixed potential theory applies to electroless plating systems as well. An explanation of this phenomenon is proposed on the basis of the mixed potential theory.

Application of the mixed potential theory [11] has led to a technique by which electroless plating processes may be classified according to their overall mechanisms. The observation of the behavior of the mixed potential as opposed to the traditional methods of polarization curves has several advantages, including freedom from *IR* drop and simplicity of measurement.

### Application of the mixed potential theory

An electroless plating process is a perfect example of two or more reactions occurring simultaneously at the same electrode. The anodic reaction is the decomposition of the reducing agent,

$$R^0 \to R^{z+} + ze^-. \tag{1}$$

and the cathodic reaction the reduction of the metal complex

$$M^{z+} + ze^{-} \rightarrow M^{0}. \tag{2}$$

A condition necessary for electroless plating to occur is that the equilibrium potential for the reducing agent  $E_{\rm R}^0$  is more cathodic than the corresponding potential  $E_{\rm M}^0$  for the metal deposition reaction. At equilibrium, the Wagner-Traud postulate applies and the plating rate,  $i_{\rm plating}$ , is given by

$$i_{\text{plating}} = i_{\text{R}} = |i_{\text{M}}|, \tag{3}$$

where  $i_R$  and  $i_M$  are the anodic and cathodic partial currents (with opposite signs). The potential associated with this dynamic equilibrium condition is referred to as the mixed

potential  $E_{\mathrm{MP}}$ . The value of the mixed potential lies between  $E_{\mathrm{R}}^0$  and  $E_{\mathrm{M}}^0$  and depends on parameters such as exchange current densities  $i_{\mathrm{R}}^0$  and  $i_{\mathrm{M}}^0$ , Tafel slopes  $b_{\mathrm{R}}$  and  $b_{\mathrm{M}}$ , temperature, etc. The mixed potential corresponds to two different overpotentials

$$\eta_{R} = E_{MP} - E_{R}^{0} \tag{4}$$

and

$$\eta_{\mathsf{M}} = E_{\mathsf{MP}} - E_{\mathsf{M}}^{0} \,. \tag{5}$$

If a current is passed through the cell, the measured currentpotential curve is the algebraic sum of the partial currentpotential curves for each electrode reaction.

Electroless plating of metals can involve a reaction that proceeds at a rate limited by diffusion. For example, the plating rate of copper in a copper-formaldehyde bath is determined, to a large extent, by the rate of diffusion of copper ions to the plating surface [12]. The technique described here allows a clear distinction between those reactions whose rate is controlled by the rate of diffusion of reactants to the plating surface, and those reactions whose rate is limited by some slow electrochemical step. The first type of reaction is said to be under diffusion control, and the second is said to be under electrochemical control.

In order to achieve conditions of controlled mass transfer, the measurements were performed using a rotating disk electrode (RDE). The current due to the diffusion of metal ions to such a geometrical surface is given [13] by

$$|i_{\mathsf{M}}| = B_{\mathsf{M}}'(C_{\mathsf{M}}^{\infty} - C_{\mathsf{M}}^{\mathsf{a}}) \sqrt{\omega}, \tag{6}$$

where  $C_{\mathbf{M}}^{\infty}$  is the bulk concentration of the reducing agent,  $C_{\mathbf{M}}^{\mathbf{a}}$  is the surface concentration, and  $B_{\mathbf{M}}'$  is a diffusion parameter given [13, 14] by

$$B_{\rm M}' = 0.62 \ n_{\rm M} F D_{\rm M}^{2/3} \ v^{-1/6} \ A. \tag{7}$$

The symbols are defined in the Appendix at the end of the paper. For diffusion-controlled cathodic partial reaction,  $C_{\rm M}^{\rm a}=0$ , and the limiting current  $i_{\rm M}^{\rm D}$  is independent of potential and takes the form

$$(1) \quad |i_{\mathsf{M}}^{D}| = B_{\mathsf{M}}^{\prime} C_{\mathsf{M}}^{\infty} \sqrt{\omega} \,. \tag{8}$$

Similarly, the diffusion-limited current for the anodic partial reaction is

$$(2) \quad i_{\rm R}^{\rm D} = B_{\rm R}^{\prime} C_{\rm R}^{\infty} \sqrt{\omega} \,. \tag{9}$$

The concentration of metal ions at the surface may be expressed by the Nernst equation

$$E_{\rm M} = E_{\rm M}^0 + \frac{RT}{n_{\rm M}F} \ln C_{\rm M}^a, \tag{10}$$

which, when Eq. (6) and Eq. (8) are substituted, becomes

$$E_{M} = E_{M}^{0} + \frac{RT}{n_{M}F} \ln |(i_{M}^{D} - i_{M})| - \frac{RT}{n_{M}F} \ln B_{M}' - \frac{RT}{n_{M}F} \ln \sqrt{\omega}.$$
 (11)

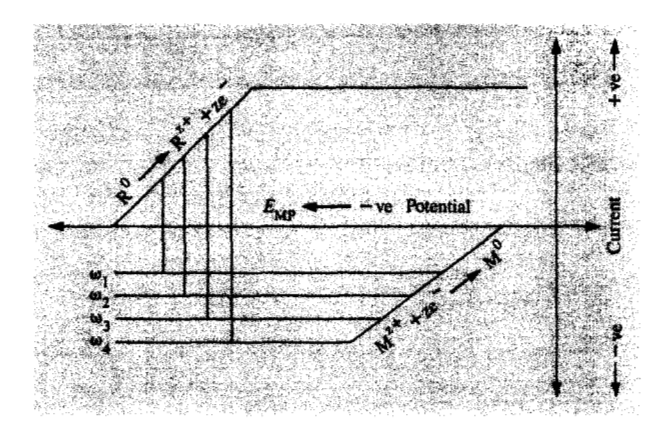


# Figure 1

Symbolic representation of the overall reaction scheme for electroless metal deposition in which the cathodic partial reaction is diffusion-controlled and the anodic partial reaction is activationcontrolled.

The corresponding equation for the reducing agent can also be worked out in a similar manner.

When the anodic partial reaction is under electrochemical control, the polarization curve is described by the equation

$$E = E_{\rm R}^0 - b_{\rm R} \ln i_{\rm R}^0 + b_{\rm R} \ln i_{\rm R}. \tag{12}$$

The anodic Tafel slope  $b_R$  is given by

$$b_{\rm R} = \frac{RT}{(1 - \alpha_{\rm R})n_{\rm R}F}.$$
 (13)

Similarly, when the metal deposition reaction is activationcontrolled, the kinetics are described by the cathodic Tafel equation

$$E = E_{\rm M}^{0} + b_{\rm M} \ln |i_{\rm M}^{0}| - b_{\rm M} \ln |i_{\rm M}|, \tag{14}$$

where

$$b_{\rm M} = \frac{RT}{\alpha_{\rm M} n_{\rm M} F}.$$
 (15)

If each partial reaction is either under electrochemical control or under mass transfer control, the overall reaction scheme consists of four hypothetical combinations. These are considered next and the dependence of  $E_{\rm MP}$  on experimental parameters, such as rotation rate  $\omega$  and  $C_{\rm R}^{\infty}$  and  $C_{\rm M}^{\infty}$ , determined.

Case 1 Cathodic partial reaction is diffusion-controlled: anodic partial reaction is electrochemically controlled.

The diffusion-limited cathodic partial current depends on  $C_{\rm M}^{\infty}$ ,  $D_{\rm M}$ , and  $\omega$ , and its magnitude is given by Eq. (8). Then using Eq. (3) to combine Eq. (8) with Eq. (12), which describes the anodic partial reaction, gives

$$E_{\rm MP} = E_{\rm R}^0 - b_{\rm R} \ln i_{\rm R}^0 + \frac{b_{\rm R}}{2} \ln B'_{\rm M}^2 \omega + b_{\rm R} \ln C_{\rm M}^{\infty}. \tag{16}$$

Equation (16) shows that the mixed potential is a linear function of  $\ln \omega$  and  $\ln C_{\rm M}^{\infty}$  and that the Tafel slope for the anodic partial reaction may be obtained by plotting  $E_{\rm MP}$  against either of these experimental parameters. Similar functions have been obtained by Makrides [15] for corrosion processes. Case 1 is represented graphically in the symbolic diagram of Figure 1. Oxygen or air is frequently bubbled through electroless copper baths to oxidize any Cu(I) species formed and thus avoid bath decomposition via Cu(I) disproportionation. Under these circumstances there is another cathodic current due to oxygen reduction, and the total cathodic current is the sum

$$i'_{M} = i_{M} + i_{O_{2}},$$
 (17)

where  $i_{O_2}$  is the current for oxygen reduction. At the plating potential  $i_{O_2}$  is diffusion-limited; that is, it is independent of the electrode potential and therefore equivalent to a cathodic current applied externally.

Under the circumstances Eq. (8) becomes

$$|i_{\mathbf{M}}^{D'}| = (B_{\mathbf{M}}^{\prime}C_{\mathbf{M}}^{\infty} + B_{\mathbf{O}_{2}}^{\prime}C_{\mathbf{O}_{2}}^{\infty})\sqrt{\omega},$$
 (8')

and Eq. (16) becomes

$$E_{MP} = E_{R}^{0} - b_{R} \ln i_{R}^{0} + b_{R} \ln (B_{M}^{\prime} C_{M}^{\infty} + B_{O_{2}}^{\prime} C_{O_{2}}^{\infty}) + \frac{b_{R}}{2} \ln \omega.$$
 (16')

Therefore the diagnostic criteria for Case 1 remain unchanged in the presence of oxygen in the plating bath.

Case 2 Cathodic partial reaction is electrochemically controlled: anodic partial reaction is diffusion-controlled.

This is the converse of Case 1, so that the cathodic and anodic partial reactions are described by Eq. (9) and Eq. (14), respectively. Combining these with the help of Eq. (3) yields

$$E_{\rm MP} = E_{\rm M}^0 + b_{\rm M} \ln |i_{\rm M}^0| - \frac{b_{\rm M}}{2} \ln B_{\rm R}^{\prime 2} \omega - b_{\rm M} \ln C_{\rm R}^{\infty}.$$
 (18)

Once again  $E_{\mathrm{MP}}$  is linearly dependent on  $\ln \omega$  and  $\ln C_{\mathrm{R}}^{\infty}$ .

The slope of  $E_{\rm MP}$  vs ln  $\omega$  plot is negative, thus making it easily distinguishable from Case 1. It can easily be shown that, in the presence of oxygen in the plating solution, the form of Eq. (18) does not change.

Case 3 Both partial reactions are electrochemically controlled.

Case 4 Both partial reactions are diffusion-controlled.

Cases 3 and 4 are rarely encountered in electroless plating baths. Therefore, detailed relationships between the mixed potential and other parameters are not worked out. Suffice it to say that in both these cases the mixed potential is independent of rotation rate.

# **Experimental procedures**

All measurements were performed in a glass cell under conditions of controlled mass transport using the rotating disk electrode technique. The working electrode was a 0.458-cm² copper disk embedded in a cylinder of Teflon (trademark of E. I. du Pont de Nemours & Co., Inc., Wilmington, DE). The working electrode and the rotator were fabricated by Pine Instruments. The counter electrode was a gold foil of large surface area and the potential was monitored with respect to an Ag/AgCl cell and a saturated calomel (SCE) reference electrode. Electrochemical measurements were performed with a PAR 173 Potentiostat in conjunction with a PAR 175 Universal Programmer. The data were recorded with the aid of a Yokogawa X-Y-T recorder.

Activation of the copper electrode was necessary for the mixed potential measurements. This was achieved by immersing the electrode first in 3% HNO $_3$  for 30 seconds followed by immersion for four minutes in  $2.26\times10^{-3}$  M PdCl $_2+1\%$  HCl. The electroless plating baths were synthesized principally from Analar grade chemicals. The experimental formulation of the electroless bath used in the present investigation is as follows: copper sulfate pentahydrate (variable), EDTA (variable), 0.0784 M formaldehyde; pH and temperature are as noted in the figure captions.

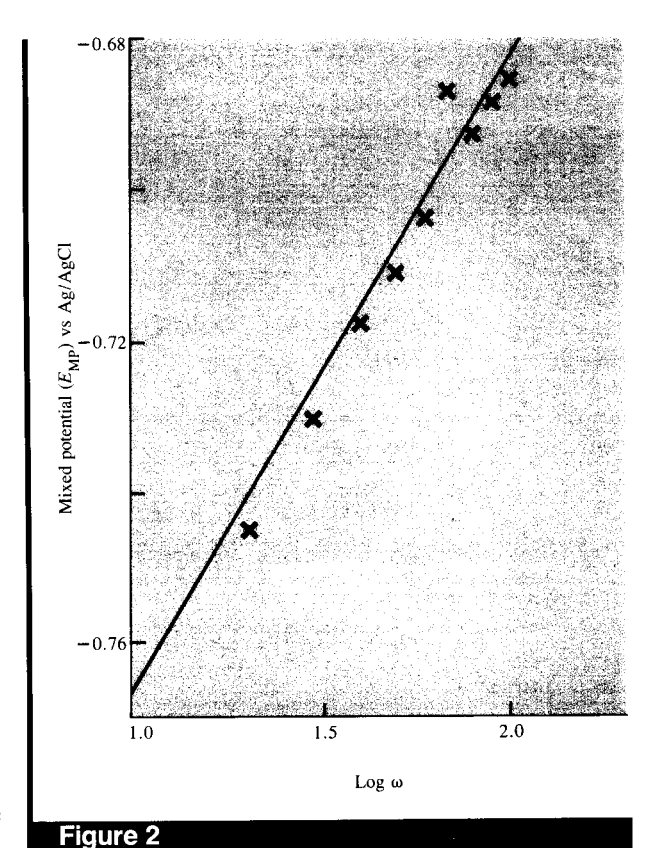
Polarization curves for the partial reactions were obtained separately in the catholyte and the anolyte. The methods used included potential scanning and the potential step and galvanostatic step techniques. The catholyte consisted of all the bath components except formaldehyde and the anolyte consisted of all bath components except copper sulfate. However, for the formaldehyde oxidation/reduction measurements approximately a millimoler amount (0.08 M) of sodium formate was also added to the anolyte.

# **Experimental results and discussion**

In an effort to confirm the interdependence of the partial reactions, measurements were performed in the complete electroless copper bath as well as in the catholyte and in the anolyte separately.

# • Behavior of mixed potential

The overall mechanism of copper plating was determined by the technique that is based on the application of the mixed potential theory to a rotating disk electrode and is described in the second section. The mixed potential was observed as a function of rotation rate,  $\omega$ , of the RDE and the bulk concentrations  $C_{\rm M}^{\infty}$  of metal ions. The data obtained are shown in Figures 2 and 3. The slopes of these straight lines were determined by least-squares analysis. Using the criteria developed earlier, it is relatively simple to assign a mechanism to the electroless plating process. We first note that the mixed potential increases with both rotation rate  $\omega$ 



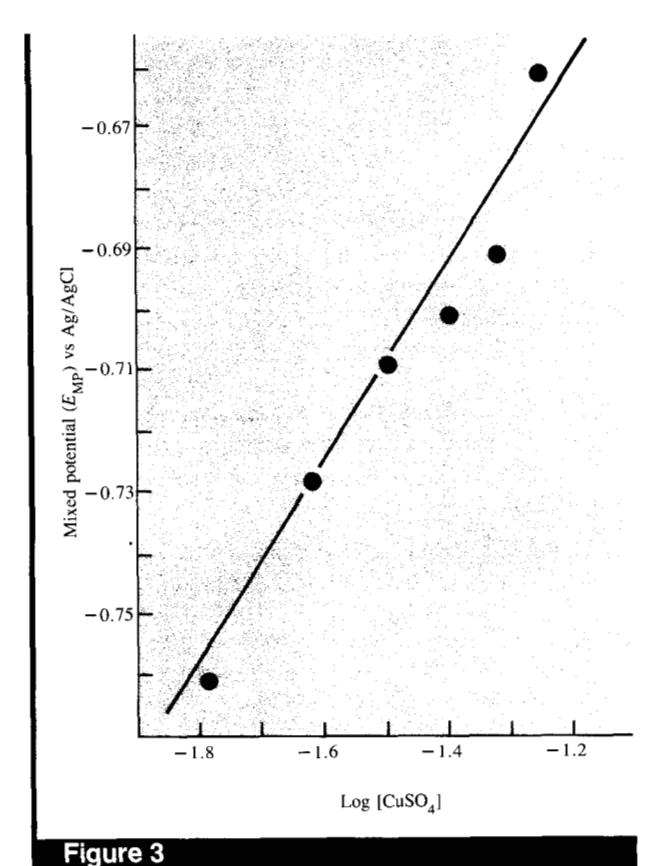
Plot of the mixed potential of the plating solution as a function of rotation rate. Temperature =  $70^{\circ}$ C; pH = 11.7.

and the concentration,  $C_{M}^{\infty}$ , of metal ions in the plating bath; that is, the slopes for the plots in Figs. 2 and 3 are positive. This behavior is indicative of diffusion-controlled copper deposition partial reaction and activation-controlled formaldehyde decomposition reaction. The same mechanism with respect to the copper deposition partial reaction has been noted previously by Donahue [12].

Verification of the theory developed for this technique is obtained by comparing the measured slope of the rotation rate dependence,  $dE_{\rm MP}/d\ln\omega$ , with the concentration dependence  $dE_{\rm MP}/d\ln C_{\rm M}^{\infty}$ . These slopes are reported in Table 1, which shows that

$$\frac{dE_{\rm MP}}{d\ln C_{\rm M}^{\infty}} = 2 \times \frac{dE_{\rm MP}}{d\ln \omega} = b_{\rm r}. \tag{19}$$

This result is predicted by Eq. (16) of the theory developed in the second section. Clearly, this simple technique is capable of measuring in situ the Tafel slope for either the anodic partial reaction or the cathodic partial reaction, depending on the overall mechanism of the plating process. In the electroless copper bath under study in this investigation,  $b_c$  is the Tafel slope for formaldehyde



A plot of the mixed potential of the plating solution against the logarithm of the  $CuSO_4$  concentration. Temperature = 70°C; pH = 11.7.

 Table 1
 Analysis of formaldehyde oxidation data: log of current density vs potential.

Method	Electrolyte	Slope/mV	Transfer coefficient
$dE_{MP}/d\log\omega$	Complete bath	104	0.34
$dE_{MP}/d \log [HCHO]$	Complete bath	210	0.33
$dE_{MP}/d \log [CuSO_4]$	Complete bath	188	0.37
$dE_{MP}/d \log i_{R}$ (galvanostatic)	Complete bath	185	0.38
$dE_{MP}/d \log i_{R}$ (galvanostatic)	Anolyte	110	0.64
$\frac{dE_{MP}/d\log i_{R}}{(\text{potentiostatic})}$	Anolyte	115	0.61
$\frac{dE_{MP}/d\log i_{M}}{(\text{galvanostatic})}$	Complete bath	$-30 \pm 5$	0.43
$dE/d \log i_{\rm M}$ (potential scanning)	Catholyte	-165	0.42

oxidation and has the value ~+210 mV/decade at 70°C. In order to further substantiate the validity of this approach, galvanostatic step measurements were also performed in the

electroless copper bath. The Tafel plot obtained is shown in Figure 4. The Tafel slope obtained has the value of +185 mV/decade at 70°C, which is in reasonable agreement with the value obtained by the technique based on the observation of the behavior of the mixed potential. This latter technique is therefore important, not only from the point of view of ascertaining the overall mechanism of electroless metal plating; it is also a convenient method for determining the Tafel slope for the partial reaction under electrochemical control.

Tafel slopes in the range of 185 to 210 mV/decade correspond to values of the anodic transfer coefficient,  $(1 - \alpha_R)n_R$ , which are substantially lower than 0.5 (Table 1, Column 4). The observed value of the transfer coefficient is known to deviate from 0.5 when the actual electron transfer occurs across only a fraction of the Helmholtz double layer, i.e., when the reacting species are specifically adsorbed and the electron transfer occurs in the inner Helmholtz plane [16]. Such behavior is characteristic of catalytic reactions. The large value of the Tafel slope implies control by the first electron transfer under Temkin adsorption conditions. Under the circumstances, the oxidation of formaldehyde in electroless copper plating may be derived from the following set of reactions:

Scheme A

$$HCHO + H_2O \rightleftharpoons H_2C(OH)_2$$
, (A1)

$$H_2C(OH)_2 + (OH^-)_{ads} \rightleftharpoons [H_2C(OH)O^-]_{ads} + H_2O,$$
 (A2)

or

$$HCHO + (OH^{-})_{ads} \rightleftarrows [H_{2}C(OH)O^{-}]_{ads},$$
 (A3)

$$[H2C(OH)O-]ads \rightleftharpoons HCOOH + \frac{1}{2}H2 + e-,$$
 (A4)

$$HCOOH + OH \rightleftharpoons HCOO + H_2O.$$
 (A5)

Formaldehyde in aqueous solutions exists predominantly in the electroinactive hydrated form. Reaction (A1) above represents the quasi-equilibrium of the hydration reaction at high pH values. The anion of the hydrated form, which is the electroactive species, can then be created either in the bulk solution by a general base catalysis [17] or can be generated on the substrate surface by interaction with adsorbed OH as shown in reactions (A2) and (A3). The high value of the Tafel slope indicates a catalytic reaction and therefore supports the participation of the substrate surface, either as an antecedent step to the electron uptake or as a proceeding step to stabilize reaction intermediates [18, 19]. Measurements performed here do not allow a distinction as to whether the hydrogen abstraction in reaction (A4) precedes the electron uptake or follows it. Nonetheless, reaction (A4) is the rate-determining step (rds) in the overall mechanism. The overall stoichiometry of the reaction is in agreement with that proposed by Lukes [20]. The mechanism of formaldehyde oxidation on metals with

different hydrogen overpotential is described in detail in Part II of this paper [21].

Further support for the validity of the mixed potential technique can be found in the Tafel curve for the copper deposition partial reaction obtained in the complete bath (**Figure 5**). The Tafel slope observed in this case has a value of  $-30 \pm 5$  mV/decade. For pure diffusion control by metal ions in the plating bath, the Tafel equation may be written as [22]

$$|E - E_{\mathbf{M}}^{0}| = \frac{RT}{2F} \ln \left(1 - \frac{i_{\mathbf{M}}}{i_{\mathbf{M}}^{D}}\right).$$
 (20)

At potential values where  $i_{\rm M} \ll i_{\rm M}^D$ , Eq. (20) reduces to the usual form of the Tafel equation,

$$|E - E_{\rm M}^{0}| = a' - \frac{RT}{2F} \ln |i_{\rm M}|,$$
 (21)

where the term a' is different from the term a in the Tafel equation [cf. Eq. (23)]. Equation (21) exhibits a Tafel slope of -37 mV/decade at  $70^{\circ}\text{C}$ , suggesting that the cathodic partial reaction in the electroless copper process is diffusion-controlled.

There are two possible mechanisms by which this could occur. These are (1) rate-controlling diffusion of  $[CuEDTA]^{2-}$  to the substrate followed by dissociation of the complex prior to reduction, and (2) dissociation of the  $[CuEDTA]^{2-}$  complex in the bulk solution followed by rate-controlling diffusion of aqueous copper ions to the substrate for reduction. The techniques used in this investigation do not allow a distinction between these two mechanisms. In either case the rate of reduction of copper ions is much faster than the rate at which electrons are released by the reducing agent. The fact that the cathodic partial reaction in electroless copper plating is diffusion-controlled is in total agreement with the overall mechanism for electroless copper plating ascertained by observing the behavior of the mixed potential as a function of  $\omega$  and  $C_M^{\infty}$ .

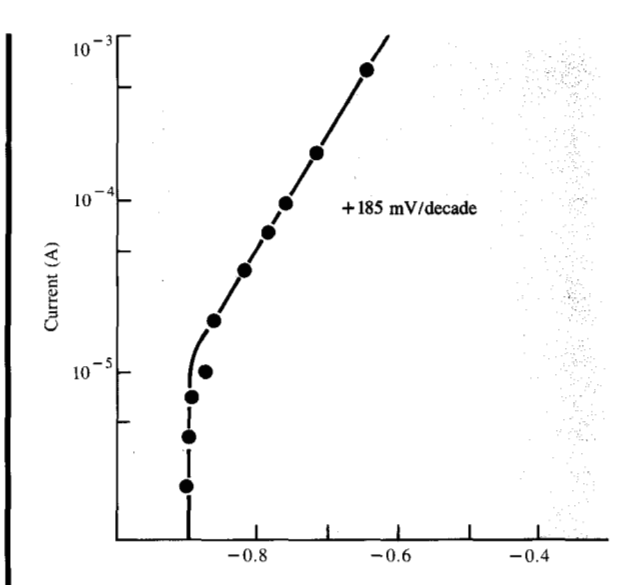
## Cathodic partial reaction

Some typical results for the copper deposition partial reactions in the catholyte are shown in **Figures 6**, **7**, and **8**. The polarization curves obtained by applying the potential scanning technique at various rotation rates are displayed in Fig. 6. If the kinetics are first order with respect to copper ions in solutions, then the experimental disk currents are related to the rotation rate by the Levich equation (13) where all quantities are considered as positive:

$$\frac{1}{i_{\rm M}} = \frac{1}{i_{\rm M}^{\rm k}} + \frac{1}{i_{\rm M}^{\rm D}} = \frac{1}{i_{\rm M}^{\rm k}} + \frac{1}{B_{\rm M}\sqrt{\omega}} \,. \tag{22}$$

It is clear from Eq. (22) and Eq. (8) that  $B_{\rm M} = B_{\rm M}' C_{\rm M}^{\infty}$ .

Figure 7 depicts plots of  $1/i_{\rm M}$  vs  $1/\sqrt{\omega}$  for the data shown in Fig. 6. These plots are linear and parallel, indicating that the copper deposition reaction is first order in copper ion



Mixed potential (V) vs Saturated Calomel Electrode (SCE)

# Figure 4

Polarization curve for formaldehyde oxidation obtained in the complete bath by the galvanostatic pulse method. Temperature =  $70^{\circ}$ C; pH = 11.7.

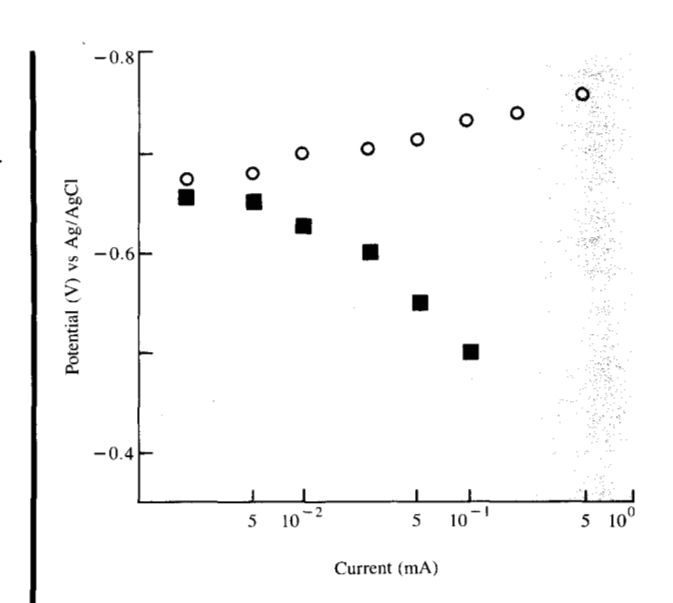
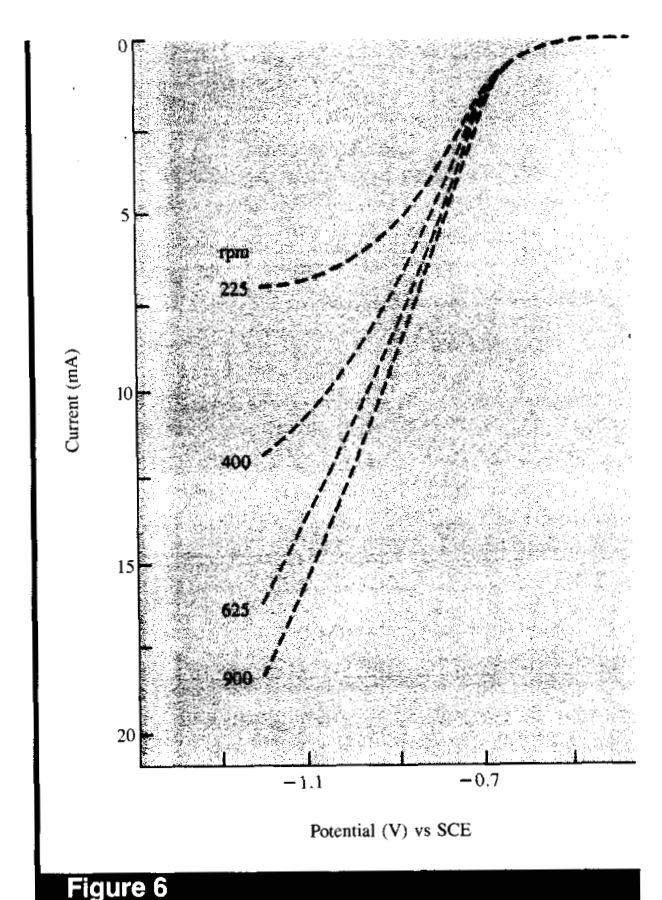


# Figure 5

Polarization curves for copper deposition (o) and formaldehyde oxidation (■) obtained in the complete bath by the galvanostatic pulse method. Temperature = 70°C; pH = 11.7.

concentration. Figure 8 shows a mass-transfer corrected Tafel plot at 70°C. There is a large linear region which yields a Tafel slope of -165 mV/decade. The value of the transfer



Rotating disk data for copper deposition in the catholyte at  $70^{\circ}$ C. Electrode area =  $0.458 \text{ cm}^2$ .

coefficient,  $\alpha_{\rm m}$ , calculated from this slope comes to 0.42. The polarization curve for copper deposition in the complete bath was also obtained and is shown in Fig. 5. This plot was obtained by the galvanostatic step method and yields a Tafel slope of  $-30~{\rm mV/decade}$ .

For a multistep, *n*-electron transfer deposition reaction, Eq. (21) may be written in the form

$$|E - E_{M}^{0}| = a - b_{M} \ln |i_{M}|,$$
 (23)

where  $b_{M}$  is given by Eq. (15) and  $a_{M}$  is expressed as [23]

$$\alpha_{\mathbf{M}} = \left(\frac{\gamma}{\nu} + n_{\mathbf{M}}\beta_{\mathbf{M}}\right). \tag{24}$$

In Eq. (24),  $\gamma$  is the number of preceding steps prior to the rate determining step and  $\nu$  the stoichiometric number;  $n_{\rm M}$  and  $\beta_{\rm M}$  are defined in the Appendix at the end of the paper. The various pathways by which copper deposition in the catholyte may occur are as follows:

$$[CuEDTA]^{2^{-}} + 2e^{-} \rightleftharpoons Cu^{0} + EDTA^{4^{-}}, \tag{I}$$

 $[CuEDTA]^{2-} + e^{-} \xrightarrow{rds} [CuEDTA]^{3-} + e^{-} \rightleftharpoons$ 

$$Cu^0 + EDTA^{4-}$$
, (II)

$$[CuEDTA]^{2^{-}} + e^{-} \rightleftharpoons [CuEDTA]^{3^{-}} + e^{-} \stackrel{rds}{\longrightarrow}$$

$$Cu^{0} + EDTA^{4^{-}}. \quad (III)^{-}$$

One need only identify the values of r,  $\nu$ ,  $n_{\rm M}$ , and  $\beta_{\rm M}$  in order to determine the mechanism of copper deposition. Mechanism I is rejected on the grounds that a two-electron transfer would require a very high activation energy. Also, a  $\beta_{\rm M}$  value of 0.21 obtained from Eq. (24) for Mechanism I is unlikely. For Mechanism III, Eq. (24) gives a  $\beta_{M}$  value which is negative and therefore has no physical meaning. Hence copper deposition in the catholyte occurs via Mechanism II, i.e., in two steps with the cupric-cuprous step as the rds. In the presence of cyanide ions in the catholyte, it is possible that the cuprous ion is stabilized by complexation with the cyanide. Such a mechanism was not investigated in this study. It is interesting to note, however, that the mechanism of copper deposition in the catholyte is similar to the mechanism postulated for copper deposition from CuSO<sub>4</sub> solutions [24].

# ♠ Anodic partial reaction

The oxidation of formaldehyde in the analyte was investigated by the galvanostatic and the potentiostatic step

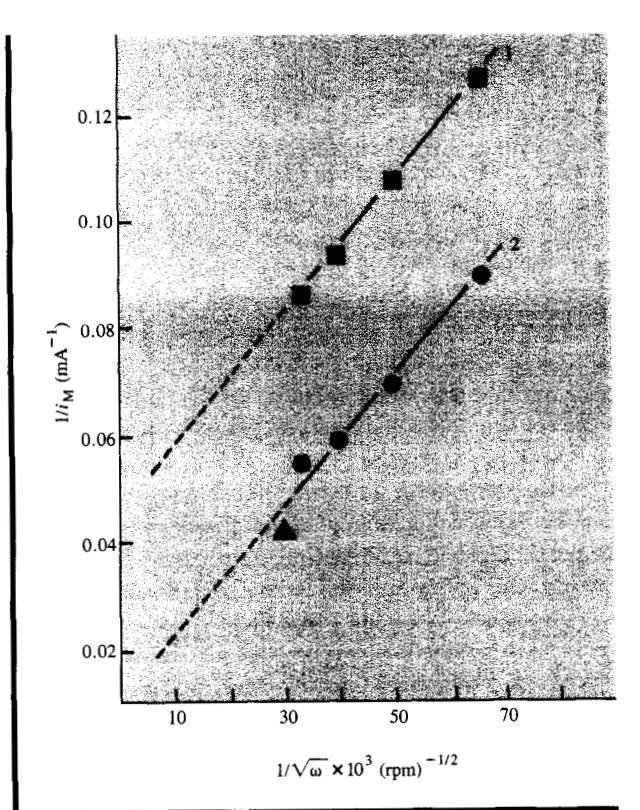


Figure 7

Plots of  $1/i_{\rm M}$  vs  $1/\sqrt{\omega}$  for the RDE data from Fig. 6. (1) -0.8 V; (2) -0.95 V.

methods (Figure 5 and Figure 9). Logarithmic analysis of the data gives linear plots of  $\log i$  as a function of potential with Tafel slopes which are considerably lower than those obtained in the complete electroless copper bath (Table 1). Such low Tafel slopes can be interpreted only in terms of a complex mechanism involving chemical and electrochemical steps. The step sequence is shown in reaction scheme B.

Scheme B

$$H_2C(OH)_2 + OH^- \rightleftharpoons H_2C(OH)O^- + H_2O,$$
 (B1)

$$H_2C(OH)O^- \rightarrow HCOOH + \frac{1}{2}H_2 + e^-,$$
 (B2)

$$HCOOH + OH^{-} \rightleftharpoons HCOO^{-} + H_{2}O.$$
 (B3)

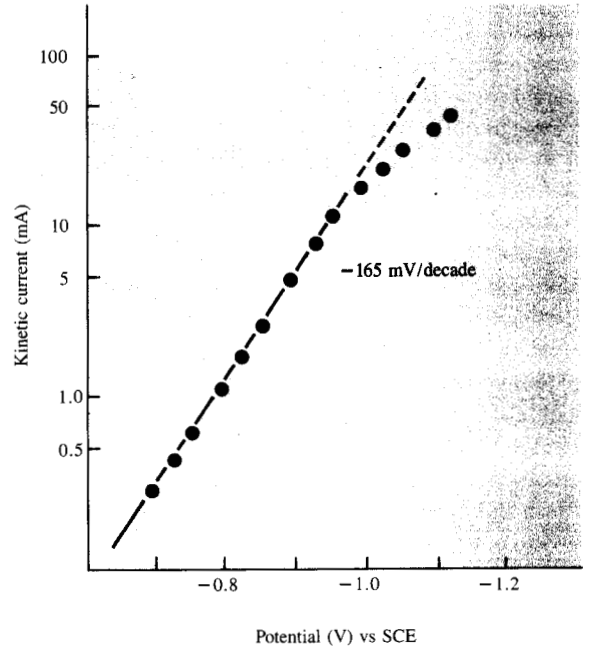
The observed Tafel slopes have a value around 110 mV/decade at 70°C (Table 1). Several reaction mechanisms could account for the experimentally observed kinetic parameters; three such mechanisms are described below.

Mechanism (i) Step (B2) is rate-controlling and the electron uptake is an inner-sphere electron transfer; i.e.,  $(1 - \alpha_R)n_R = 1$ . The Tafel slope expected (under conditions of Langmuir adsorption) if steps (B1) and (B3) are in quasi-equilibrium is then 70 mV/decade at 70°C.

Mechanism (ii) Step (B2) is the rds but the electron transfer is outer-sphere. In such a case, the Tafel slope expected under conditions of Langmuir adsorption has a value of 140 mV/decade at 70°C.

Mechanism (iii) Step (B1) is rate-determining and steps (B2) and (B3) are in quasi-equilibrium. This is quite possible since the formation of methylene glycolate anion, which is the electroactive species, is base-catalyzed and therefore depends on the pH value. A Tafel slope of 70 mV/decade at 70°C is expected in this case. However, the Tafel slope, and therefore the mechanism of formaldehyde oxidation, would then be a function of formaldehyde concentration and pH. At pH equal to the pK value for step (B1), this step is in quasi-equilibrium and mechanism (i) or (ii) outlined above becomes operative.

It is clear that the observed Tafel slope of 110 mV/decade at 70°C cannot be accounted for by only one of the mechanisms outlined above. It is possible that the components of the plating bath present in the anolyte (e.g., excess EDTA) affect formaldehyde decomposition and that the overall mechanism for this reaction is a combination of two or more mechanisms described above. In any case, it is clear that the mechanism of formaldehyde oxidation is more complex in the anolyte than in the complete plating bath, where it has been shown to be a catalytic process.



Totelliai (V)

# Figure 8

Tafel plot for copper deposition in the catholyte at 400 rpm. Temperature =  $70^{\circ}$ C; electrode area =  $0.458 \text{ cm}^2$ .

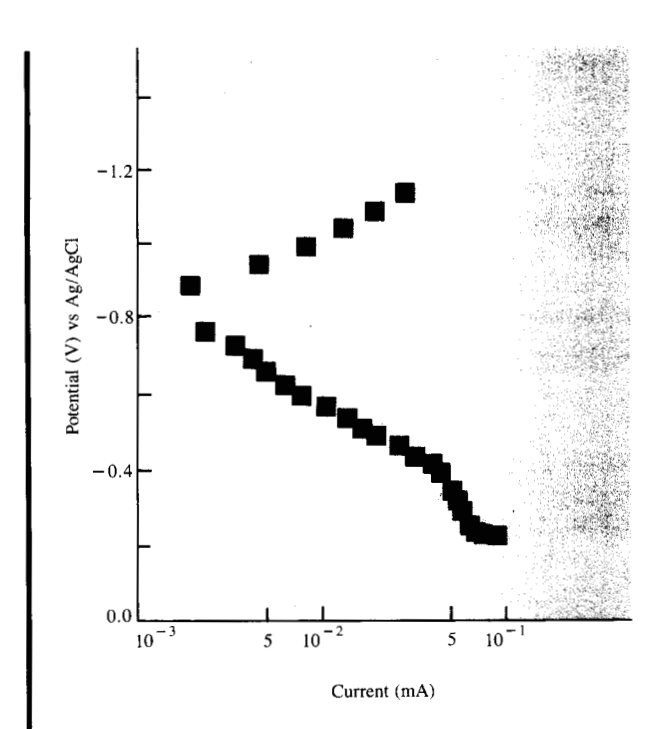


Figure 9

Polarization curves for formaldehyde oxidation and reduction obtained in the anolyte by the potentiostatic pulse method. Temperature =  $70^{\circ}$ C; pH = 11.7.

### • Interdependence of the partial reactions

To establish the interdependence or otherwise of the partial reactions in electroless copper plating, Tafel slopes for the partial reactions were obtained in the complete plating bath as well as in the catholyte and in the anolyte separately. The Tafel slope for the copper deposition reaction (Table 1) in the catholyte indicates a stepwise reaction mechanism with the cupric-cuprous step as the rds. In the electroless plating bath the Tafel slope for the cathodic partial reaction has a value of  $-30 \pm 5$  mV/decade, indicating diffusion control for this reaction. The difference in mechanisms in the catholyte and in the plating bath is attributed to the presence of the reducing agent and the anodic partial reaction in the bath. Electroless plating processes occur via two consecutive reactions. Electrons are released during the anodic partial reaction and consumed by the cathodic partial reaction, which also happens to be the metal deposition reaction. The overall rate of the electroless plating process is therefore governed by the slower of the two partial reactions. In the bath formulation studied in this investigation the exchange current density for the formaldehyde oxidation at  $E_{\rm MP}$  is at least two orders of magnitude lower than the exchange current density for the copper deposition reaction. Therefore, whatever the mechanism of copper deposition in the catholyte, the electroless plating process is controlled by the kinetics of the formaldehyde oxidation reaction; i.e., the rate of the copper deposition partial reaction is totally dependent on the kinetics of the anodic partial reaction. Hence the two partial reactions in electroless copper plating are not independent of each other.

Further evidence in support of this theory is provided by the Tafel plots for formaldehyde oxidation in the plating bath and in the analyte (Table 1). There is considerable difference in Tafel slopes in the two solutions, indicating a difference in the mechanism of the reaction in the two environments. Clearly, the anodic partial reaction in the electroless plating bath is affected by the presence of copper ions in the bath.

# **Conclusions**

The interdependence of partial reactions in electroless plating processes has been demonstrated. It has been shown that the overall mechanism of an electroless plating process can be determined by observing the behavior of the mixed potential as a function of agitation, concentration of metal ions, or concentration of reducing agent, if the partial reactions are either under diffusion control or electrochemical control. In general, partial reactions may also be under mixed control, but the theory developed thus far suggests that a vigorous treatment which would take such reactions into account would be very involved. Hence partial reactions under mixed control have been ignored here.

In conclusion, it should be emphasized that the technique and the theory developed in this paper can be used to

ascertain the overall mechanism of an electroless deposition reaction only if the partial reactions are either under diffusion control or under electrochemical control. In the case of electroless copper plating, for instance, it has been shown that the formaldehyde partial reaction is electrochemically controlled while the metal deposition partial reaction is diffusion-controlled, but in order to obtain complete validity for the technique it would be necessary to apply it to several other electroless plating systems.

# Appendix: List of symbols

$\boldsymbol{A}$	Electrode	area

 $b_{\mathbf{R}}$ 

Tafel slope intercept a

Diffusion parameter for CuEDTA<sup>2-</sup> complex  $B'_{M}$ 

 $B_{\mathrm{O_2}}'$ Diffusion parameter for dissolved oxygen

 $B_{\mathbf{R}}'$ Diffusion parameter for HCHO

 $b_{\mathbf{M}}$ Tafel slope for cathodic partial reaction

Tafel slope for anodic partial reaction

 $C_{\mathbf{M}}^{\infty}$ Bulk concentration of copper ions

 $C_{\mathbf{o_2}}^{\infty}$ Bulk concentration of dissolved oxygen

 $C_{\mathbf{R}}^{\mathbf{a}}$ Surface concentration of HCHO

 $C_{\mathbf{R}}^{\infty}$ Bulk concentration of HCHO

 $D_{\mathbf{R}}$ Diffusion coefficient of HCHO

Ε Electrode potential

 $E_{\mathsf{M}}$ Thermodynamic reversible potential for the metal deposition reaction

 $E_{\mathbf{M}}^{0}$ Standard electrode potential for copper deposition

 $E_{MP}$ Mixed potential

Thermodynamic reversible potential for reducing agent reaction

 $E_{R}^{0}$ Standard electrode potential for HCHO

Faraday constant

 $i_{\mathbf{M}}$ Current density for metal deposition

 $i'_{\mathbf{M}}$ Total cathodic current density

Kinetic controlled current density for metal

deposition

 $i_{\mathbf{M}}^{0}$ Exchange current density for metal deposition

Diffusion-limited current density for metal

deposition

Diffusion-limited current density for total cathodic reactions

Current density for oxygen reduction  $l_{O_2}$ 

Plating current density

l<sub>plating</sub>

Current density for HCHO oxidation

Exchange current density for HCHO oxidation

Diffusion-limited current density for HCHO

oxidation

- $n_{\rm M}$  Number of electrons transferred in metal deposition reaction
- $n_{\rm R}$  Number of electrons transferred in the HCHO oxidation reaction
- R Gas constant
- T Absolute temperature
- ν Stoichiometric number
- $\alpha_{\rm M}$  Transfer coefficient for metal deposition
- $\alpha_R$  Transfer coefficient for HCHO oxidation reaction
- $\beta_{\rm M}$  Symmetry factor
- $\gamma$  Number of preceding steps prior to rds
- $\eta_{\rm M}$  Overpotential for metal deposition
- $\eta_R$  Overpotential for HCHO oxidation reaction
- v Kinematic viscosity
- $\omega$  Rotation rate of rotating disk electrode

### References

- C. Wagner and W. Traud, "The Interpretation of Corrosion Phenomena by Superimposition of Electrochemical Partial Reactions and the Formation of Potentials of Mixed Electrodes," Z. Electrochim. 44, 391 (1938).
- J. V. Petrocelli, "The Electrochemical Behavior of Aluminum, I. In Solutions of Cerium Sulfate in Sulfuric Acid," *J. Electrochem. Soc.* 112, 124 (1965).
- 3. E. J. Kelly, "The Active Iron Electrode, I. Iron Dissolution and Hydrogen Evolution Reactions in Acidic Sulfate Solutions," *J. Electrochem. Soc.* 112, 124 (1965).
- M. Paunovic, "Electrochemical Aspects of Electroless Deposition of Metals," *Plating* 51, 1161 (1968).
- S. M. El-Raghy and A. A. Aho-Solama, "The Electrochemistry of Electroless Deposition of Copper," J. Electrochem. Soc. 126, 171 (1979).
- F. M. Donahue and F. L. Shippey, "Kinetics of Electroless Copper Plating. II. Mixed Potential Analysis," *Plating* 60, 135 (1973).
- F. M. Donahue and C. U. Yu, "A Study of the Mechanism of the Electroless Deposition of Nickel," *Electrochim. Acta* 15, 237 (1970)
- A. Molenaar, M. F. E. Holdrinet, and L. K. H. van Beek, "Kinetics of Electroless Copper Plating with EDTA on the Complexing Agent for Cupric Ions," *Plating* 61, 238 (1974).
- 9. F. M. Donahue, "Interactions in Mixed Potential Systems," *J. Electrochem. Soc.* **119**, 72 (1972).
- T. N. Andersen, M. H. Ghandehari, and M. Ejuning, "A Limitation to the Mixed Potential Concept of Metal Corrosion, Copper in Oxygenated Sulfuric Acid Solutions," *J. Electrochem.* Soc. 122, 1580 (1975).
- P. Bindra and J. Tweedie, "Mechanisms of Electroless Metal Plating. I. Application of the Mixed Potential Theory," J. Electrochem. Soc. 130, 1112 (1983).
- F. M. Donahue, "Kinetics of Electroless Copper Plating. III. Mass Transport Effects," J. Electrochem. Soc. 127, 51 (1980).
- V. G. Levich, *Physicochemical Hydrodynamics*, Prentice-Hall, Inc., Englewood Cliffs, NJ, 1962.
- A. C. Riddiford, Advances in Electrochemistry and Electrochemical Engineering, Vol. 4, Interscience Press, New York, 1966.
- A. C. Makrides, "Dissolution of Iron in Sulfuric Acid and Ferric Sulfate Solutions," J. Electrochem. Soc. 107, 869 (1960).
- D. S. Gnanamuthu and J. V. Petrocelli, "A Generalized Expression for the Tafel Slope and the Kinetics of Oxygen Reduction on Noble Metals and Alloys," *J. Electrochem. Soc.* 114, 1036 (1967).

- D. Barnes and P. Zuman, "Polarographic Reduction of Aldehydes and Ketones XV: Hydration and Acid-Base Equilibrium Accompanying Reduction of Aliphatic Aldehydes," J. Electroanal. Chem. 46, 323 (1973).
- D. Manousek and J. Volke, "Anodic Oxidation of Aromatic Aldehydes at Mercury Electrodes," J. Electroanal. Chem. 43, 365 (1973).
- 19. W. Vielstich, *Fuel Cells*, D. J. G. Ives (trans.), Wiley-Interscience Publishers, London, 1970.
- R. M. Lukes, "The Chemistry of the Autocatalytic Reduction by Copper by Alkaline Formaldehyde," *Plating* 51, 1066 (1964).
- Perminder Bindra, Judith M. Roldan, and Gary V. Arbach, "Mechanisms of Electroless Metal Plating: II. Decomposition of Formaldehyde," *IBM J. Res. Develop.* 28, 679–689 (1984, this issue).
- K. J. Vetter, Electrochemical Kinetics, Academic Press, Inc., New York, 1967.
- J. O'M. Bockris and A. K. N. Reddy, Modern Electrochemistry, Vol. 2, MacDonald & Co. Ltd., London, 1970.
- 24. U. Bertocci and D. R. Turner, Encyclopedia of Electrochemistry of the Elements, Vol. 2, Marcel Dekker, New York, 1974.

Received March 20, 1984; revised June 15, 1984

Perminder Bindra IBM Research Division, P.O. Box 218, Yorktown Heights, New York 10598. Dr. Bindra is currently manager of two groups in the area of electrochemistry and metal plating in the Manufacturing Research Center at Yorktown Heights. These groups are involved in fundamental studies in electrochemistry as well as in studies designed to understand the deposition characteristics of metals such as copper, nickel, gold, and bimetallics of the permalloy family, and in developing monitors and process controls for electroless and electrolytic plating solutions. He joined IBM in 1979 in the Research Division. Dr. Bindra received the Ph.D. in electrochemistry from the University of Southhampton in London, England, in 1973. From 1974 to 1977, he was a postdoctoral fellow at the Max-Planck Institut in Berlin, West Germany. Prior to joining IBM, he was on the chemistry faculty at Case-Western Reserve University. In 1983, Dr. Bindra's work on electroless and electrolytic copper plating was recognized with an IBM Outstanding Technical Achievement Award. He has also received two IBM Invention Achievement Awards.

David N. Light IBM Research Division, P.O. Box 218, Yorktown Heights, New York 10598. Mr. Light graduated Phi Beta Kappa from Stanford University, California, in 1979, receiving a B.A. in human biology. He subsequently performed research at the Woods Hole Marine Biological Laboratory and the Smithsonian Institution's Chesapeake Bay Center for Environmental Studies,

before joining IBM in 1981. He is now a senior associate engineer in the Manufacturing Research Center, where he is investigating the electrochemistry of metal plating and the properties of plated films. He is also involved in the development of monitors for plating bath components. Mr. Light has received a Research Division Award and an Invention Achievement Award from IBM for his work in these areas.

**David L. Rath** *IBM Research Division, P.O. Box 218, Yorktown Heights, New York 10598.* Dr. Rath received his B.S. in physics in 1971 at St. John's University, Collegeville, Minnesota, and his Ph.D. in physics in 1978 at Utah State University, Logan. From 1979 to 1981 he held the position of guest scientist at the Fritz-Haber-Institut in Berlin, West Germany, where he investigated the properties of the immersed electrochemical interface. From 1981 to 1982, he was a postdoctoral fellow at Ames Laboratory, U.S. Department of Energy, Ames, Iowa, where he was involved in a collaborative effort to characterize the photoelectrochemical processes of layered semiconductors. Dr. Rath joined IBM in 1982 as a research staff engineer, in which capacity he is presently investigating the adsorption characteristics of additives on metals and working on the design and development of plating bath monitors.